Evolution in Electrical and Electronic Engineering Vol. 3 No. 1 (2022) 271-281

EEEE

Homepage: http://publisher.uthm.edu.my/periodicals/index.php/eeee
e-ISSN : 2756-8458

Statistical Analysis of Frequency Response Collected on Fault Stator Winding in Three Phase Induction Motor

Zeachter Witjoanes[1], Mohd Fairouz Mohd Yousof [1]*

[1]Faculty of Electrical and Electronic Engineering,
Universiti Tun Hussein Onn Malaysia, Parit Raja, Batu Pahat, 86400, MALAYSIA

*Corresponding Author Designation

DOI: https://doi.org/10.30880/eeee.2022.03.01.031
Received 20 January 2022; Accepted 10 April 2022; Available online 30 June 2022

Abstract: Electric motors are the most used electrical machines in the industry. The three-phase induction motors (TPIM) are commonly used for conveyors, compressors, elevators, etc. However, TPIM can be prone to a variety of problems that cause motor malfunctions also failures and the most important part is the stator windings. This paper is about using three types of statistical indicators (SIs) such as Correlation Coefficient (CC), Absolute Sum of Logarithmic Error (ASLE), and Root Mean Square Error (RMSE) to detect the frequency response's deformation on fault stator windings. The data was collected from a previous literature review that used frequency response analysis (FRA) in TPIM with various faults stator windings. This paper aims are to simulate the frequency responses (FRs) using statistical indicators (SIs) and propose a benchmark limit for one of the SI. Thus, the simulated frequency response is compared with the measured frequency response of a normal winding condition and faulty winding motor condition. The proposed method has shown SIs are useful to detect winding deformation in TPIM.

Keywords: Frequency Response Collected, Fault Stator Winding, Induction Motor

1. Introduction

Asynchronous machines, often known as induction machines, are the most widely utilized electrical machinery in the industry. In TPIM, it has two main parts which are the stator and rotor, these two need to be in perfect condition to work perfectly and efficiently. The failure mechanisms of induction motors vary based on components such as the rotor, stator, and shaft, the most important of which is the stator winding [1]. The stator windings' fault is usually the main reason why the TPIM failed to work perfectly, stator and rotor faults will damage the internal of the motor such as coil-to-coil connections, sever overload, and physically damaged coils [2]. According to a study conducted by the Electric Power Research Institute (EPRI), stator winding problems account for 36% of motor failure [3, 4]. The percentage of induction motor failures recorded as a result of this category ranged from almost 30% to 40% [5].

Corresponding author: fairouz@uthm.edu.my

In power transformers, FRA is a powerful and responsive tool for measuring the mechanical integrity of transformer cores, windings, and press frames [6]. The FRA can also be used in TPIM to detect the frequency response's deformation on fault stator windings. FRA can be represented by using statistical indicators (SIs), by using this interpretation and validation for the FR, it can distinguish between the normal stator winding response before and after the fault stator winding occurred.

In this paper, the FRA was performed on TPIM with various winding fault conditions such as phase turn-to-turn fault (PTT), phase coil-to-coil fault (PCC), phase-to-ground fault (PTG), phase coil-to-ground fault (PCG), and open circuit fault (OCF), the data collected from the paper is used in this paper [7]. SIs data simulated using coding, were analyzed and determined which SIs has much more sensitivity when detecting the deformation of stator winding faults.

2. Materials and Methods

2.1 Method

Figure 1 shows the flowchart of the project.

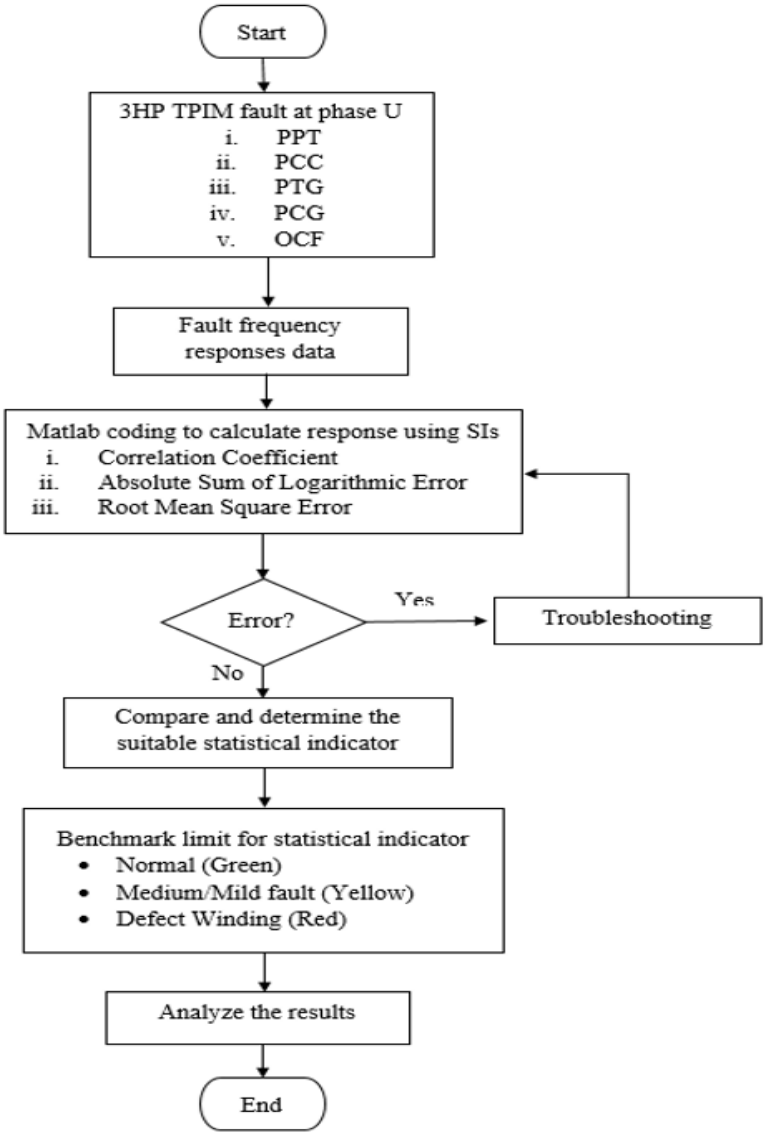

Figure 1: Flowchart of the project

The first stage required understanding the theory of TPIM and searching the information from journals, thesis, and online resources about the fault in stator windings. Next, find out the coding based on SIs for Correlation Coefficient (CC), Absolute Sum of Logarithmic Error (ASLE), and Root Mean Square Error (RMSE). From the coding simulated, the FR has plotted as well as SIs all at the same time. If the coding simulation succeeded, then can proceed to compare all SIs which one is the most sensitive to detect FR during normal and faulty windings' conditions. After that, benchmark limits will be proposed to determine the response limit which region will be normal windings (green), medium/mild fault windings (yellow), and defect windings (red). The responses and SIs will be analyzed and discussed in the final stage of this paper.

2.2 Three-Phase Induction Motor

In this paper, an artificial fault in stator winding was created using 3HP TPIM JILANG 90L-2 to simulate a real-life fault in the stator winding. This motor was chosen because of the Wye (Y) connection arrangement between phases U, V, and W, which is extensively utilized for TPIM. The specification of TPIM is shown in Table 1.

Table 1: Specification of TPIM [8]

Specification of TPIM	
Manufacturer	JILANG
Model	Y90L-2
Phases	3-ph induction motor
Power	2.2kW / 3HP
Rated Voltage	415V / 50Hz
RPM	2840 rpm

2.3 FRA Measurement Connection

Figure 2 shows the measure connection made using FRA, computer, and TPIM tested with various faults at phase U. The winding connection configuration, which is Wye (Y), was used to define the measuring process. FRA responses of Wye-connected windings can be measured between two-phase terminals (U-V, V-W, and W-U) or phase to neutral terminals (U-N, V-N, and W-N), however the neutral point (N) is assumed hidden in this case because this paper was conducted only on (U-V, V-W, and W-U). Various faults were created such as PTT, PCC, PTG, PCG, and OCF. The FRA responses were measured between phase terminals (U-V, V-W, and W- U) and the response measurement was recorded inside Microsoft Excel.

Figure 2: FRA cable connection to measured FRA in TPIM [8]

2.4 Frequency Regions

On the FR curve, three frequency regions were created, as shown in Figure 3. These regions are positioned in a specific frequency range, which must be specifically based on the response wave shape. The magnitude response of a tested TPIM obtained using FRA is mostly in the frequency domain, implying that each frequency range is related to the motor transfer function. The transfer function itself

indicates the response from each complex parameter inside the TPIM. In this project, the FRA generated is between 200 Hz and 1 MHz. Three frequency ranges low frequency (LF), medium frequency (MF), and high frequency (HF) have been established to reveal various types of faults' responses.

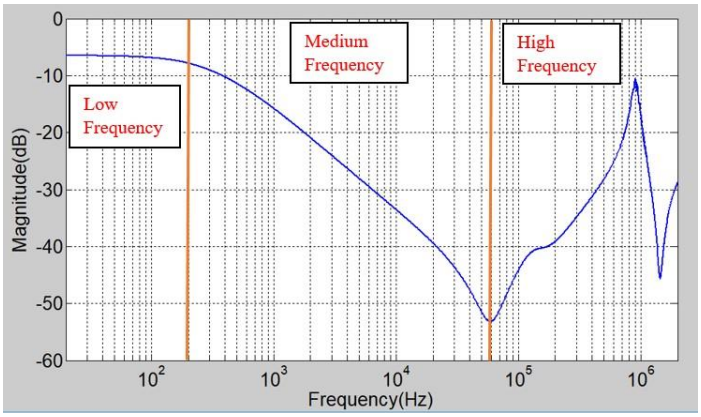

Figure 3: Frequency regions for normal condition TPIM

2.5 MATLAB Coding Flowchart

Figure 4 shows the paper coding flow.

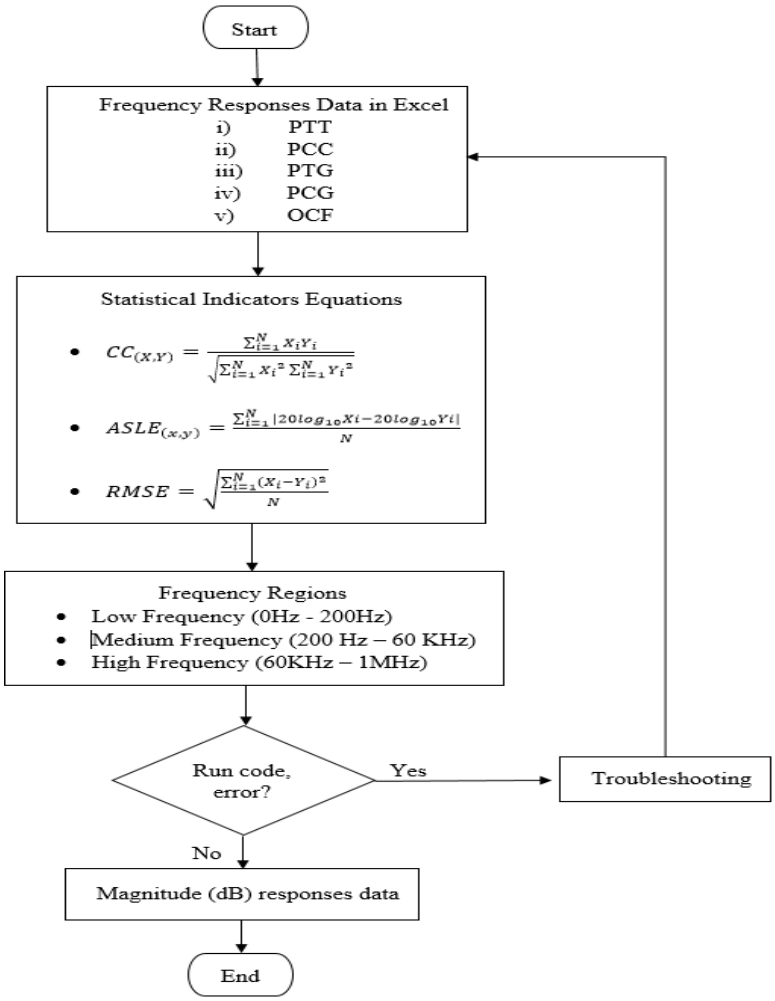

Figure 4: Coding flow for stator winding responses

All of the FRA test measurement data for TPIM 3HP was measured using FRANEO 800 and the data was then recorded in Microsoft Excel. The coding was written so that the data from FRA test measurements in Excel can be imported into MATLAB. Various faults such as PTT, PCC, PTG, PCG, and OCF of it was tested between different phases of windings. The equations in coding are the representation of statistical data for FRA that gives a value of variables to show the relationship that exists between two variables' relative movements. Frequency regions were divided into three regions LF, MF, and HF, these frequency regions are to analyze the stator winding's responses with various fault conditions from LF to HF region.

3. Results and Discussion

3.1 Frequency Responses All Types of Faults on Stator Windings

Frequency responses were compared between normal and fault condition motor. The three responses were tested on terminal U-V, V-W, and W-U. There are five faults' condition performed which are PTT, PCC, PTG, PCG, and OCF but only two of these faults PTT and OCF were used for comparison to show different fault deformation.

3.1.1 Phase turn-to-turn fault (PTT) frequency responses

Figure 5 shows that FR for phase U-V was not the same with a normal condition motor. It can be seen that the starting magnitude for both motor's conditions is the same but when the frequency region increases from medium to high-frequency region, the fault was detected with a minor gap between each other.

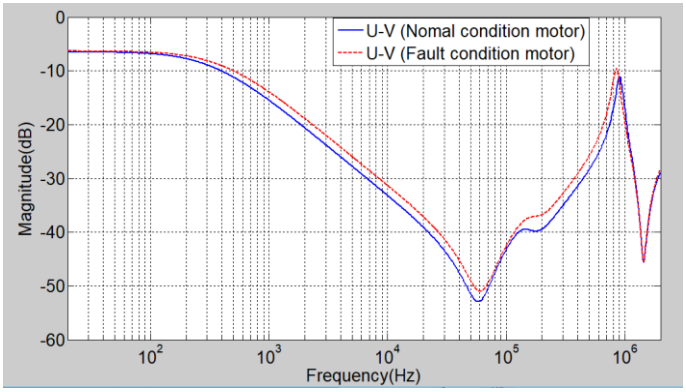

Figure 5: FRA during normal and PTT fault conditions for phase U-V

Figure 6 shows that FR at phase V-W was identical. The starting magnitude of the fault condition motor is similar to the normal condition motor. From the responses above It can be seen clearly that the graph of simulated PTT fault stator winding did not affect the phase V-W. All of the frequency regions were similar to the normal condition stator winding

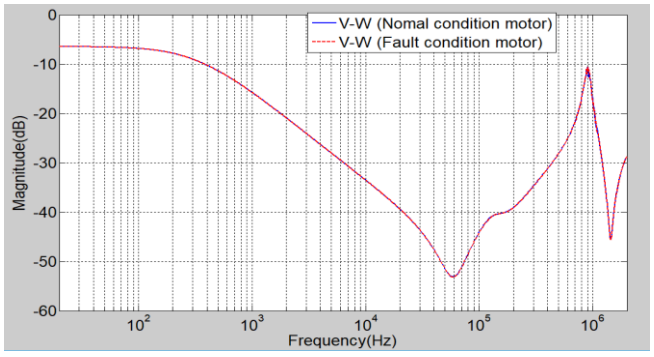

Figure 6: FRA during normal and PTT fault condition for phase V-W

Figure 7 shows that FR for phase W-U was almost similar to frequency responses from phase U-V. In the HF region, there is a gap difference between phase W-U and U-V.

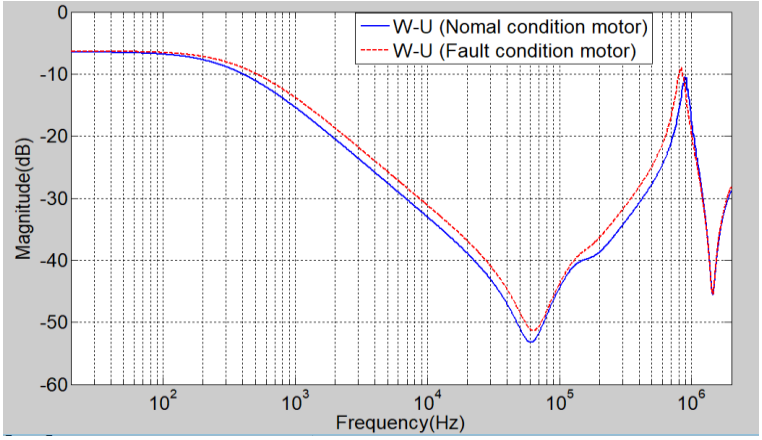

Figure 7: FRA during normal and PTT fault condition for phase W-U

Table 2 show the results of all SIs tested in PTT fault at phase-U. In this case, there is a fault occurring at phase U-V and phase W-U while phase V-W shows normal condition and a small defect in the winding. CC at phase V-W showed a value of 1.0000 dB meaning that it is a perfect match. It can be seen that the fault winding started from the MF region showed a gap with a value above 1.5000dB. ASLE and RMSE at phase U-V and phase W-U shows values above 2.0000 during the HF region. This huge value represented that phases U-V and W-U was defective stator windings and need to do future investigation on the motor. This fault was typically caused by contaminants, abrasion, vibration, or voltage surge

Table 2: PTT fault frequency responses by using CC, ASLE, and RMSE

Frequency region	Frequency responses in dB of 3HP motor								
	CC			ASLE			RMSE		
	U-V	V-W	W-U	U-V	V-W	W-U	U-V	V-W	W-U
Below to 200 Hz (low sub-band)	0.9999	1.0000	0.9999	0.2887	0.0018	0.2975	0.3076	0.0019	0.3161
200 Hz to 60kHz (Medium sub-band)	0.9999	1.0000	0.9999	1.6544	0.0044	1.6998	1.7127	0.0070	1.7631
60 kHz to 1MHz (High sub-band)	0.9989	1.0000	0.9987	2.1694	0.0441	2.2247	2.4146	0.1308	2.4241

3.1.2 Open Circuit Fault (OCF) Frequency Responses

Figure 8 shows a major fault in the stator winding, the fault condition motor's magnitude is far from the normal condition motor. The fault stator windings will drop its power by about half and the motor will not start. The test motor's internal connection is multi-circuit it can start but with reduced power,

because of the open circuit windings, it will cause the magnetic circuit to be unbalanced. This motor will run the load more slowly and eventually overheat making the windings more damaged.

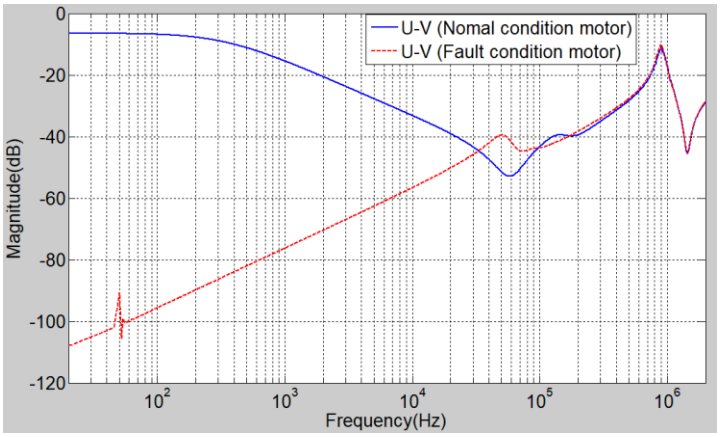

Figure 8: FRA measurement for 3HP TPIM at normal condition and OCF for phase U-V

Figure 9 shows the fault condition motor was matching with the normal condition motor because there is no fault created at phases V and W.

Figure 10 shows an identical result as phase U-V, at LF region the magnitude was very high this shows the stator winding is in major fault. At MF region, the deformation started to decrease until HF region.

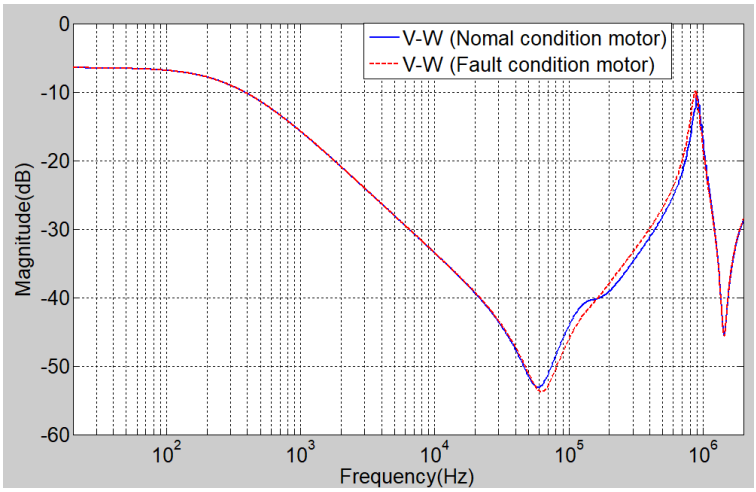

Figure 9: FRA measurement for 3HP TPIM at normal condition and OCF for phase V-W

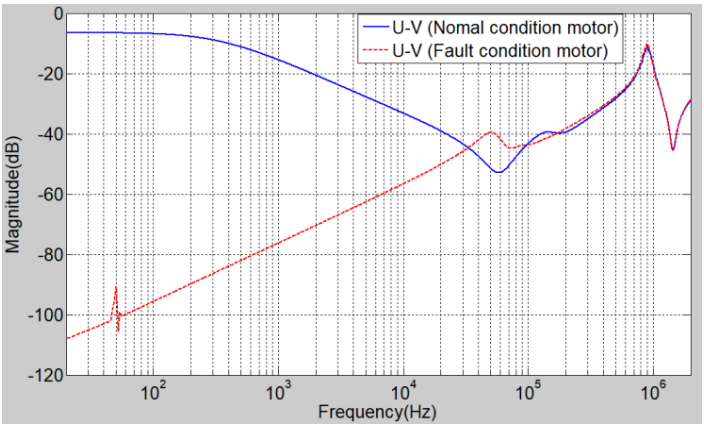

Figure 10: FRA measurement for 3HP TPIM at normal condition and OCF for phase W-U

Table 3 shows the simulation results that have different values in all SIs tested in open circuit fault at phase-U. In this case, phase results at U-V and W-U show a major defect in TPIM. The motor still needs proper rewinding at phase U because prolonging this issue will damage the motor even more. All of the indicator's values show fault during starting of the motor. CC shows a reading of 0.7766 dB at phase U-V, when CC drops below 1.0000 dB it indicates the stator windings faced faults. ASLE and RMSE show a huge values' gap at phase U-V and W-U which is above 89.0000 dB during the LF region and 40.0000 dB during the MF region. Both of these indicators at phase V-W show very low responses which are 0.0018 dB and 0.0023dB. During HF region, the magnitude has decreased below1.6300 dB for ASLE and 2.6200 for RMSE. From the indicators, the stator windings faced serious fault and need to be investigated.

Table 3: OCF fault frequency responses by using CC, ASLE, and RMSE

Frequency region	Frequency responses in dB of 3HP motor								
	CC			ASLE			RMSE		
	U-V	V-W	W-U	U-V	V-W	W-U	U-V	V-W	W-U
Below to 200 Hz (low sub-band)	0.9953	1.0000	0.9954	89.0158	0.0018	89.0759	89.1558	0.0023	89.2151
200 Hz to 60kHz (Medium sub-band)	0.7766	1.0000	0.7768	40.8382	0.0570	40.9260	47.8893	0.1226	47.9776
60 kHz to 1MHz (High sub-band)	0.9981	0.9991	0.9980	1.6233	1.4284	1.2493	2.4922	1.5111	2.6172

3.2 Statistical Indicators Comparison

Three statistical indicators have been used to compare frequency responses and each indicator shows a different range sensitivity value when detecting fault windings. It is likely that under certain circumstances, either these parameters aren't sensitive to existing variations in the data. From all of the fault results, the response above 1MHz did not affect the winding deformation. Below shows PCC and OCF bar chart frequency responses without dividing it into three frequency regions.

Figure 11 shows the difference in FR value for CC was not significant between both windings' conditions meaning that it is not suitable to use as SI because from the value itself person is hard to determine whether the TPIM is in normal condition or fault winding condition. SIs for ASLE and RMSE can be seen that there is a noticeable difference when the TPIM is in both windings' conditions. Both of the indicators have a value above 1.5000 dB during winding deformation, at normal winding conditions, the value for ASLE is much lower which is 0.0262 compared to RMSE which is 0.1064. The percentage difference between these two statistical indicators at deformation winding during phase U-V, and W-U is 14.77% and 15.94%, as for CC it is 0.08% which is really small, and it highlights that CC's deficiency in these types of faults. Results indicate that the damage sensitivity for the RMSE has slightly increased

during both of the phases, it can be said that these two indicators are really useful to detect winding deformation.

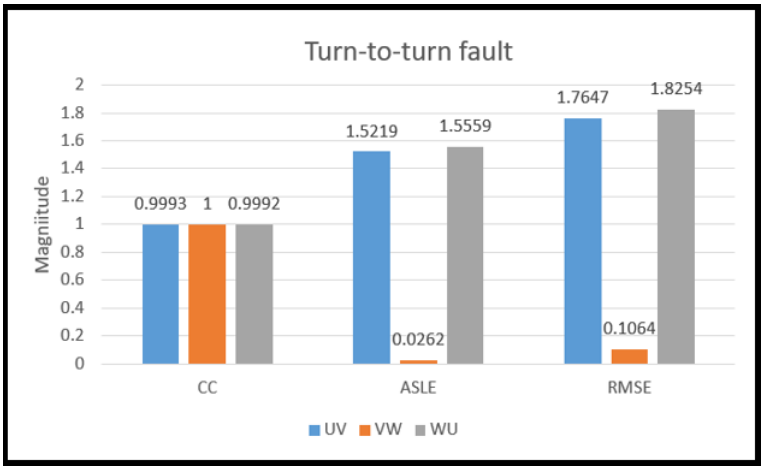

Figure 11: Bar chart frequency responses for PTT

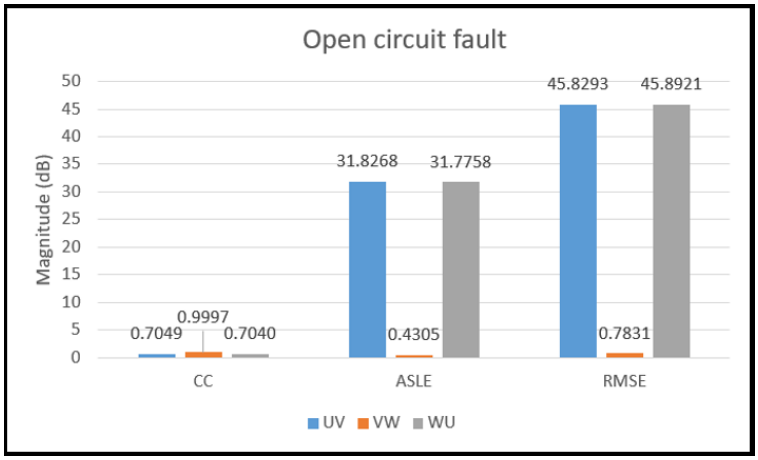

Figure 12: Bar chart frequency responses for OCF

OCF is the most deform winding result compared to all of the other types of faults. Figure 12 as above shows that there is a large deviation difference in all of the statistical indicators, thus ASLE and RMSE can be compared much more precisely because of the huge deformation result. Both of these indicators faced a major winding deformation at phase UV and WU with a reading above 31.5000dB for ASLE and 45.5000 dB for RMSE. Although CC did not have significant changes in magnitude, during OCF, it decreased a lot until below 0.7050 dB. The percentage differences for all indicators during deformation winding faults are 29.48 % for CC, 36.06% for ASLE, and 36.35% for RMSE. From the overall results gathered, during the LF region, both of the indicators ASLE and RMSE do not really affect the frequency of responses. The response is noticeable when both of these indicators range from MF to HF region, RMSE was much more affected from the frequency region and able to detect with much higher sensitivity for deformation windings damage. Therefore, the data which is more reliable when using SI is RMSE compared to the other two indicators, ALSE is also a good indicator, but it is not consistent when changing to a higher frequency.

3.3 Benchmark Limits of Statistical Indicator

A Benchmark limit indicator will be proposed for RMSE based on the analysis when comparing all indicators. Since the response winding deformation is very sensitive compared with other indicators, these findings proposed a benchmark limit as shown in Table 4.

Table 4: Proposed indicator benchmark limit

Condition	RMSE
Normal	0 dB - 1.5 dB
Mild fault	1.5 dB - 2.5 dB
Defect	above 2.5 dB

After analyzing the winding deformation responses at all frequency regions, the winding is in a normal condition when the RMSE is between 0 dB to 1.5000 dB. These can be seen during stator winding faults for PTT, PTG, and PCG, with most responses under 1.5000 dB for LF and MF regions. Windings' responses will be in mild fault conditions when it is in between 1.5000 dB to 2.5000 dB and this occur during the HF region. Defect windings that need to be investigated is when the magnitude is above 2.5000 dB, which is noticeable during the MF region for PCC and HF region for OCF. The variation is high for both of these stator windings' responses, it is above 3.5000 dB for PCC and 47.8000 dB for OCF. The deformation occurs at MF because the reduction in the number of winding coils made the winding inductance decrease. The changes in capacitance between windings U-V or W-U have had a significant impact on the response, therefore the sensitivity of the response increased as can be seen in the indicator.

4. Conclusion

Monitoring the induction motor's stator winding using FRA has helped visualize the deformation's responses, thus CC, ASLE, and RMSE were performed to evaluate the fault winding's condition in magnitude value responses. The results for both stator winding conditions were compared and noticed that each SI showed a different range of sensitivity for every frequency region. The magnitude results from all faults showed that the LF region, it had a small variation except for OCF which the magnitude was above 3.5000 dB, then when at MF region the distortion gradually increase showed the highest distortion extended until the HF region, but then it gradually decreases after responses above 1Mhz. SI was analyzed thoroughly and concluded that RMSE showed the most promising response values for stator winding's fault because of its sensitivity and consistency from lower to higher frequency regions. Benchmark limits for RMSE were made in accordance with the responses from various faults shown in the results. Normal condition motor will be between 0 dB to 1.5000 dB, for mild fault 1.5000 dB to 2.5000 dB, and defect winding will be magnitude above 2.5000 dB. These benchmark limitations are served only approximation of the stator windings' distortion and need to use various other techniques or tools that can be used to strengthen these findings.

Acknowledgement

The authors would like to thank the Faculty of Electrical and Electronic Engineering, Universiti Tun Hussein Onn Malaysia for its support.

References

[1] Zamudio-Ramirez, R. A. Osornio-Rios, M. Trejo-Hernandez, R. De Jesus Romero-Troncoso, and J. A. Antonino-Daviu, “Smart-Sensors to Estimate Insulation Health in Induction Motors via Analysis of Stray Flux,” Energies, vol. 12, no. 9, 2019, doi: 10.3390/en12091658.

[2] X. Qi, “Practical circuit design to protect motor’s phase failure operation,” in Proceedings - Asia-Pacific Conference on Power Electronics and Design, APPED 2010, 2010, pp. 104–107, doi: 10.1109/APPED.2010.34.

[3] Akar Mehmet, Ankaya Ilyas C., "Broken rotor bar fault detection in inverter-fed squirrel cage induction motors using stator current analysis and fuzzy logic," Turk J Elec Eng & Comp Sci, vol. 20, no. 1, pp. 1077–1089, 2012.

[4] Pezzani C, Donolo P., Bossio G., Donolo M., Guzman A., Zocholl S. E., "Detecting broken rotor bars with zero-setting protection," Industrial & Commercial Power Systems Technical Conference (I&CPS), IEEE/IAS 48th., pp. 1–12, 2012.

[5] G. B. Kliman, W. J. Premerlani, R. A. Koegl, and D. Hoeweler, "A new approach to on-line turn fault detection in ac motors," Proc. IEEE Industry Applications Soc. Annual Meeting Conf., San Diego, CA, pp. 687–693, 1996.

[6] “Frequency Response Analysis on Power Transformers - OMICRON.” https://www.omicronenergy.com/en/applications/power-transformer-testing monitoring/diagnosis-frequency-response-analysis-on-power-transformers/ (accessed Jan 17, 2022).

[7] A. A. Alawady, M. F. M. Yousof, N. Azis, and M. A. Talib, “Phase to phase fault detection of 3-phase induction motor using FRA technique,” Int. J. Power Electron. Drive Syst., vol. 11, no. 3, pp. 1241–1248, 2020, doi: 10.11591/ijpeds. v11.i3.pp1241-1248.

[8] A. A. Alawady, M. F. M. Yousof, N. Azis, and M. A. Talib, “Frequency response analysis technique for induction motor short circuit faults detection,” *Int. J. Power Electron. Drive Syst.*, vol. 11, no. 3, pp. 1653–1659, 2020, doi: 10.11591/ijpeds.v11.i3.pp1653-1659.